INDONESIAN MINING JOURNAL Vol. 16, No. 3, October 2013 : 132 - 148

COMPUTATIONAL ANALYSIS OF ASH EROSION ON SUPERHEATER TUBES IN COAL FIRED POWERPLANT

ANALISIS KOMPUTASI EROSI ABU PADA PIPA SUPERHEATER DALAM TUNGKU PEMBANGKIT LISTRIK BERBAHAN BAKAR BATUBARA

HAIFA WAHYU
Pusat Penelitian Fisika - Lembaga Ilmu Pengetahuan Indonesia (LIPI)
Jalan Cisitu-Sangkuriang 21/154D Bandung 40135
Phone. +62.22 2507771, Fax. +62.22 2514275
Email: wahyu@gmail.com; haifa.wahyu@lipi.go.id

ABSTRACT

This paper presents a computational analysis of fly ash erosion on superheater tubes of a coal furnace. The investigation was held based on a hypothesis that erosion by coal ash particles have caused an untimely failure of a superheater tube during the initial running of a relatively new coal fired power plant. Material erosion is usually caused by several corresponding factors, therefore, it is necessary to examine the process taken by the coal ash to wear out superheater material before conclusions on the ash factor are drawn. This work applies a combination method of analysis using mathematical model and computational fluid dynamics (CFD) simulation. The mathematical model was used to calculate the amount of erosion by the fly ash particles and CFD simulation was employed to examine the velocity profile of combustion products around the superheater bank. The CFD simulation was based on the real scale and the design parameters of the power plant. The simulation shows that the velocity vector of the combustion products around superheater bank varies from 1 to 20 m/s magnitude with impacting angle varies from 0 to 90° relative to the vertical position of the superheater. Ash data were taken from the actual coal used during the operation and the design specified coal according to the equipment specification. Mathematical model was formulated for a single ash particle and for ash bulk. The results show that differences in the ash particle parameters result in different amount of material removal which means that ash particles affect the wear out of the material. As an overall, for each ash particle, the maximum erosion occurs at impacting angle of 17°. The impacting angle is used further in determining the amount of mass removal by varying the velocity and the abrasiveness of ash particles. At the maximum level of erosion, which is the maximum velocity calculated from the CFD simulation (20 m/s), every kilogram ash particles containing 46.54 % SiO_2 with ash particle average diameter 500 micron is capable to remove about 0.0045 miligram alloy steel material. The maximum penetration of the ash particles into the superheater material is found at the maximum velocity obtained from the CFD simulation that is 20 m/s. The maximum penetration is 0.049 mm which is about 1.53 % of the pipe thickness. The superheater pipe is made of alloy steel material type A213-T91 with the thickness of pipe wall 3.2 mm. The magnitude of mass removal is considered relatively trivial to cause the thinning of material in a short period. This proves that coal ash particles will undergo a timely process to wear out superheater material, it is predictable and does not immediately cause erosion or failure. A brief physical examination was carried out to compare the results of the analysis and the causes of failures. It was found out that the failed superheater pipe had undergone clogging which caused overheating followed by pipe burst.

Keywords: coal ash, erosion, superheater tube failure, mathematical model, computational fluid dynamics simulation

Received : 19 February 2013, first revision : 12 June 2013, second revision : 25 September 2013, accepted : October 2013

SARI

Makalah ini mengemukakan analisa komputasi erosi abu batubara terhadap pipa superheater dari pembangkit listrik berbahan bakar batubara. Penelitian ini dilaksanakan dengan mengacu pada hipotesa bahwa erosi abu batubara dapat menyebabkan pecahnya pipa superheater pada saat pembangkit baru dioperasikan dimana kondisi peralatan masih dalam keadaan relatif baru. Biasanya erosi material terjadi karena beberapa faktor yang saling berhubungan. Oleh karena itu perlu dilakukan studi yang bertujuan untuk membahas proses yang terjadi saat tumbukan antara partikel abu dengan material superheater sebelum menarik kesimpulan bahwa penyebab pecahnya pipa superheater adalah karena erosi abu. Dalam studi ini, metode analisa dilakukan dengan meng-kombinasikan model matematis yang berfungsi untuk menghitung jumlah material yang tererosi serta simulasi komputasi dinamika fluida untuk mencari profil kecepatan aliran produk pembakaran batubara disekitar daerah superheater. Pipa superheater terbuat dari material baja alloy tipe A213-T91 dengan ketebalan dinding pipa 3,2 mm. Simulasi menggunakan kondisi riil dengan parameter operasi yang disesuaikan dengan spesifikasi pembangkit. Hasil simulasi memperlihatkan bahwa kecepatan aliran disekitar superheater berkisar antara 1 hingga 20 m/detik dengan sudut tumbukan antara 0-90° relatif terhadap posisi superheater yang vertikal. Data abu diperoleh dari sampel batubara yang digunakan oleh plant dan data dari dokumen spesifikasi alat. Formulasi model matematik dibuat berdasarkan individu partikel dan keseluruhan abu. Hasil dari studi ini memperlihatkan bahwa perbedaan parameter partikel batubara mengakibatkan jumlah material pipa yang terlepas akibat kena tumbukannya juga berbeda yang menunjukkan bahwa partikel batubara mengakibatkan adanya erosi dari material dinding pipa. Secara keseluruhan, untuk setiap tumbukan oleh partikel abu, erosi maksimum terhadap material yang kena tumbukan terjadi pada sudut benturan 17°. Sudut benturan ini selanjutnya digunakan dalam perhitungan jumlah erosi dari material yang terkena tumbukan dengan memvariasi kecepatan partikel abu dan tingkat abrasivitas dari partikel abu tersebut. Tingkat erosi maksimum yang dianggap berlangsung pada kece-patan maksimum yang diperoleh dari hasil simulasi CFD, yaitu 20 m/detik, untuk setiap kilogram abu batubara yang mengandung partikel SiO_2 46,54 % dengan ukuran rata-rata partikel abu 500 mikron dapat menggerus material superheater sebanyak 0,0045 mg. Penetrasi maksimum partikel abu dengan kecepatan paling tinggi hasil simulasi tersebut terhadap bahan pipa superheater adalah 0,049 mm atau sekitar 1,53 % dari ketebalan dinding pipa. Hal ini menunjukkan bahwa penipisan dinding pipa berlangsung melalui proses yang memakan waktu, dapat diprediksi dan tidak serta merta menjadi penyebab terjadinya erosi yang merusak pipa superheater. Pengamatan sepintas dilakukan terhadap kondisi pipa superheater yang pecah. Ternyata sebelumnya pipa tersebut mengalami penyumbatan yang menyebabkan adanya overheating yang diikuti pecahnya pipa.

Kata kunci: abu batubara, erosi, kegagalan pipa superheater, model matematik, simulasi komputasi dinamika fluida

INTRODUCTION

Failures in power plant boilers are due to cracks and ruptures, usually caused by prolonged over-heating which results in material thermal fatigue. Thermal fatigue occurs at one point during the life-time of any steam power plant caused by continu-ous heating and cooling process that generates transient stresses at microscopic level of boiler material. For coal fired power plants, there is an additional factor related to fly ash erosion which will cause the thinning of boiler walls and tubes and in turn leads to earlier ruptures. Thermal fatigue in boilers can be predicted based on the metal structure of boiler material, so that the replacement of the boiler materials or components can be done during scheduled time out for maintenance. How-ever, in some cases, ruptures occur in an untimely manner during normal operation of a power plant and these would cause heavy losses to the power plant operators. These untimely ruptures may be caused by excessive erosion of fly ash on boiler walls, surface deposits of corrosive materials and operational problems. The damage is usually found in superheater and reheater tube banks due to operational circumstances where temperature exceeds 650 °C, and the location of superheater where the flue gas stream turns direction.

Up to 90 % of incidents in superheaters, reheaters and wall tubes are caused by overheating (Port et al, 1991). The mounting deposit of scales slows down the coolant flow and increases the amount of heat from the fire side or burners. The prolonged exposure to excessive heat will cause the boilers operate in the temperatures above design level. Usually failures occur after a prolonged period in many tubes, start from bulging of wall followed by cracks and ruptures. The rupture caused by overheating mostly longitudinal and the edges can be thick or knifelike. To eliminate the long term overheating, the sources of deposits and improper boiler operation must be regularly identified and inspected on systems prone to be deposited such as headers, U-bends and long horizontal runs. However, overheating does not automatically produce significant tube damage. Microstructural changes cropped up in the material would also weaken the tube walls. Failures can also be associated with other attacks such as erosion from fly ash and corrosion from chemical reaction in particular oxidation. The origin of a crack is always at the point of the lowest endurance and limits the highest of local stress. Therefore a sharp corner or other surface discontinuity is critical to crack and failure. Bends in boiler tubes or erosion of turbine blades are susceptible to untimely ruptures as shown in Figures 1 and 2.

Figure 1. A rupture at the bend of a superheater tube

Studies on boiler material erosion and ruptures have been done by researchers using both experimental and mathematical model approaches. Early development of ash erosion on steel material using mathematical model was conducted by Finnie (1960). He employed the mechanisms of a cutting tool on ductile materials. In that paper, he stressed that the importance of impacting angle and velocity vector on the amount of mass removed from the impacting material. He found out that the maximum mass removal of ash velocity vector was at the angle of 18 - 20 °C. This value was consistent with the experimental results. The model was adopted by Mbabazi et al (2004) to simulate the erosion of superheater tube banks by coal fly ash. In coal-fired power stations, ash produced from the combustion of coal causes erosion, corrosion, blocking and fouling on boiler tubes and walls. Most of the fly ash particles are carried along the entrained stream of the flue gas leaving the boiler. Only a small part of the ash is deposited on the boiler walls and superheater tubes. The deposited ash is discharged during the sootblowing process as slag and clinker. Fly ash particles entrained in the gas stream from the furnace cause erosive wear on steel surfaces of the boilers and superheaters along the path. Mbabazi et al (2004) studied the effect of ash particle impacts on the erosive wear of ash particle velocity and its angle on the mild steel surfaces.

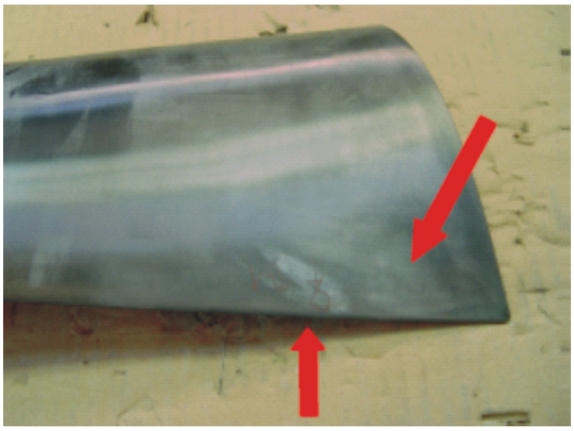

Figure 2. Erosion of a turbine blade

They used experimental investigation to examine the erosion rates caused by the collision of ash particles and the mild steel surfaces. His study on mild steel resulted in the maximum erosion occurred at 30° impacting angle. The most critical location for boiler tubes failure was in the area that subject to high temperature. In a coal furnace, the part with the highest temperature was in the horizontal area where the superheater and reheater tube banks were installed. It was found that the erosion rate was affected by impingement angles and ash velocity. If the angle of impaction was low which means the impingement angle was more slanting, then the erosion rate was high. High ash velocity also caused higher erosion rates on the boiler walls. Effect of ash from different coal quality was also observed, where the ash from lower quality coal with high silica content has the most erosive wear.

Simulation using computational fluid dynamics approach was done by Rahimi et al (2006), Vuthaluru et al (2010), Mbabazi et al (2006) and several other researchers. Rahimi et al (2006) presented a paper dealing with modeling of boiler tube ruptures using computational fluid dynamics to find the causes of the failure. The model was developed after the damage in a series of the elbows of long superheater tubes. The simulation applied continuity equations, the Reynolds-Averaged-Navier-Stokes (RANS) employing the turbulence combustion and radiation models to create temperature and pressure profiles along the tubes on a real scale. The model included the furnace walls, tubes, burners and air channels. The results of their simulation showed a difference in the temperature profile of the long tubes compared to the short tubes. The temperature difference was about 60 °C which was suspected as the major cause of the tube failures. There was a changing in the microstructure of the tube walls due to the relatively high temperature deviation examined using micro photos of the rupture. Ash related problems identification was studied by Vuthaluru et al (2010) using CFD simulation on real scale coal power plant. Temperature and flow deviation in superheater and reheater tube banks was common which can cause problems when related with ash. The study involved parameter variations based on the position of the tangentially fired burner. They found out that different position of the burners resulted in different temperature and velocity profiles at the tube banks. The objective was to study the impact of the particle trajectory and added fuel additives accordingly to reduce the problems created by ash disposition and erosion. Erosion in air heaters caused by fly ash particles has been studied by Mbabazi et al (2006) employing computational fluid dynamic approach. Simulation using CFD tool coupled with mathematical model could predict erosion on the steel surface of the air heater. The rate of erosion was dependent on the air velocity, if the air velocity was high, then the erosion rate was also high. The simulation results were verified using experimental set up by measuring the amount of wear at the steel surface, which were in agreement with the results of the simulation.

Simulation on steel tubes subject to the prolonged exposure of steel tubes to high temperature was done by Purbolaksono et al (2010) in order to prevent damage occuring prior to failures. They used finite element method to obtain profiles on temperature distribution on tube metal to enable the evaluation of the remaining life of the boiler tubes. Parameters of the operational condition were used to assess the failure using visual inspections, metallurgical examinations and mechanical strengths. Creep damage was used to estimate the lifetime of the tubes. The creep damage here was defined as the amount of life expended as time fraction. They found that the increased tube temperatures would accelerate the development of scales on the surface. There was a relationship between the hardness values and the average temperature of the tubes. The metal hardness will decrease in parallel with the increasing of metal temperature and service hours. The creep damage will therefore increase with the increase of service hours of the boiler tubes. Gong et al (2010) has studied the interaction between corrosion and erosion caused by scaling that accelerated the thinning of heat exchanger pipes and resulted in a pipe failure. Metallographic microscope and photoelectric direct reading spectrometer were used to observe the morphology and micro area compostion on the ruptured surface. The erosive effect was studied using finite element analysis. It was found that improper material selection accompanied by scaling were the major cause of the failure. Dissolved oxygen corrosion and crevice corrosion are the main factors contributing to the rupture of the tubes. The effect of deposits on boiler efficiency and performance was studied by Sandberg et al (2011) using dynamic simulation in a circulating fluidized biomass-fired boiler. Known distribution of deposits on boiler wall was used as input to the model where the heat transfer rate was reduced by half in a season. The simulation used energy and mass balances for the components in the boiler as well as a combustion model in the fluidized bed reactor. However, as an overall, the study found that the efficiency of the turbine and boiler was not affected by the fouling. This was due to the reheater that maintained the temperature and pressure within acceptable limits.

This paper presents the work on the evaluation of a sudden and untimely rupture of a superheater tube using mathematical model combined with computational fluid dynamic simulation. It was assumed that the crack of the boiler tube was caused by ash erosion. However, this has to be investigated since erosion occurs in a course of time due to several corresponding factors rather than a sudden and untimely process. Therefore, the objective of this work is to analyze the process taken by coal ash to wear superheater material.

Mathematical model was used to estimate the amount of erosion caused by ash particles. Whilst computational fluid dynamic simulation provided velocity vector and concentration profiles in a coal furnace on a full scale basis using the plant design specifications. The velocity profile was used as parameters in the mathematical model. To investigate the factor of material fatigue that already crept up in the superheater material, an analysis on the effect of yield stress variation was done to determine the relation between the amount of mass removal and the material strength. To verify the simulation results, a brief analysis on the physical condition of the failed tube was conducted.

Mathematical model used in this study was based on the model developed by Finnie (1960), since the model was found to be in line with experimental results. When a particle hit a surface, it will form an angle generating shear forces which will remove the surface of the impacting material. The amount of mass removal depends upon particle velocity, particle density and size, angle of impaction, and the type of impacting material characterized by its yield stress. Figure 3 shows the trajectory diagram of an ash particle when hitting impacting material.

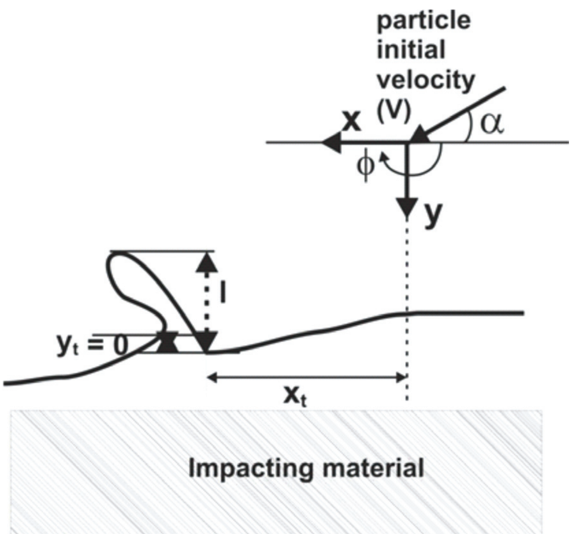

Figure 3. Ash erosion model showing the trajectory of an ash particle hit impacting material

The above diagram (Figure 3) shows the cutting model of a particle across a surface with initial velocity of V, direction ϕ and cutting angle α. The particle comes down at the cutting angle, cut the materials and leaves again. Maximum erosion occurs at lower angle α depicted in Equation 1 while higher angles depicted in Equation 2 caused the horizontal motion of the particle tip ceases while cutting. Cutting stops when the particle leaves the surface that is at $y_t = 0$.

$$Q = \frac{mv^2}{p\psi K}\left(\sin^2\alpha - \frac{6}{K}\sin^2\alpha\right) \quad \text{if } \tan\alpha \le \frac{K}{6} \;\ldots\ldots\ldots\ldots (1)$$

$$Q = \frac{mv^2}{p\psi K}\left(\frac{K\cos^2\alpha}{6}\right) \quad \text{if } \tan\alpha \ge \frac{K}{6} \;\ldots\ldots\ldots\ldots (2)$$

Q is the volume of material removed by a single ash particle with mass m and velocity V. p is the atmospheric pressure. Based on empirical studies, it was assumed that the values of ψ = 2 and K = 2 (Finnie et al, 1978), therefore the volume removal of angular abrasive grains is rearranged into the following equations (Equations 3 and 4) according the following conditions:

$$Q = \frac{MV^2}{8p}\left(\sin^2\alpha - 3\sin^2\alpha\right) \quad \text{if } \tan\alpha \le 18.5° \;\ldots\ldots (3)$$

$$Q = \frac{MV^2}{24p}\left(cos^2\alpha\right) \quad \text{if } \tan\alpha \ge 18.5° \;\ldots\ldots\ldots\ldots (4)$$

M is the total mass of ash particles. For angles close to maximum erosion, Finnie et al (1978) simplified Equations 3 and 4 to become:

$$Q \approx 0.075\left(\frac{MV^2}{24p}\right)\frac{1}{p} \;\ldots\ldots\ldots\ldots (5)$$

The model developed by Mbabazi et al (2004) employed the deep of penetration on the impacting material shown in Equation 6.

$$m_p\frac{d^2h}{dt^2} = -\pi\frac{d_p}{2}hc\sigma_y \;\ldots\ldots\ldots\ldots (6)$$

The depth of penetration equals h, particle mass m_p, particle density ρ_p and particle diameter d_p, t is the time, σ_y the yield stress of the target material, and c is a particle shape factor equal to 3 for a sphere. Hence, for a sphere particle, mp becomes:

$$m_p = \frac{1}{6}\rho_p\pi d_p^3 \;\ldots\ldots\ldots\ldots (7)$$

The negative sign denotes the resistance toward the penetrating action by the particle. Substituting Equation 7 into Equation 6 results in Equation 8 written as follows.

$$\frac{d^2h}{dt^2} = -\frac{9\sigma_y h}{\rho_p d_p^2} \quad \text{.......... (8)}$$

The maximum penetration occurs at h_{max} when dh/dt = 0, which is presented by the Equation 9:

$$h_{max}^3 = \frac{d_p^3}{3^3} V^3 \sin^3\alpha \left(\frac{\rho_p}{\sigma_y}\right)^{3/2} \quad \text{.......... (9)}$$

Therefore the mass of the material removed is proportional to the above equation as shown below.

$$m = K_c \rho_m h_{max}^3 = \frac{K_c \rho_m \rho_p^{3/2} d_p^3 V^3 \sin^3\alpha}{3^3 \sigma_y^{3/2}} \quad \text{.......... (10)}$$

where ρ_m is the density of the target material, ρ_p is the density of the impacting particle, and d_p is particle density. Hence, the ratio of the mass removal relative to the impacting particle can be represented in the following equation.

$$\varepsilon_c = \frac{m}{m_p} = \frac{K_1 \rho_m \rho_p^{1/2} V^3 \sin^3\alpha}{\sigma_y^{3/2}} \quad \text{..........(11)}$$

Mbabazi et al. (2004) also included plastic deformation in its erosion rate presented in the following equation.

$$m = K_p \rho_m h_{max}^3 = \frac{K_p \rho_m \rho_p^{1/2} d_p^3 V^3 \sin^3\alpha}{H_v^{3/2}} \quad \text{........ (12)}$$

H_v is Vickers hardness number of the impacting material which was related to the stress yield.

$$H_v = 2.7\,\sigma_y \quad \text{.......... (13)}$$

The relative plastic deformation for each particle is given in the following equation.

$$\varepsilon_p = \frac{m}{m_p} = \frac{K_2 \rho_m \rho_p^{1/2} V^3 \sin^3\alpha}{H_v^{3/2}} \quad \text{.......... (14)}$$

The total mass removal (ε) was the combination of material removal and plastic deformation resulting in Equation 15.

$$\varepsilon = \frac{K x^{4.95} \rho_m \rho_p^{1/2} V^3 \sin^3\alpha}{\sigma_y^{3/2}} \quad \text{.......... (15)}$$

K is the total constant, x is the mass fraction of silica contained in the ash.

If the impacting material has been in load cycles, the material endurance will be reduced shown by the decrease in the capacity of the material to absorb the maximum stress (Figure 4) (Boardman, 1990). This will also reduce the yield stress of the material.

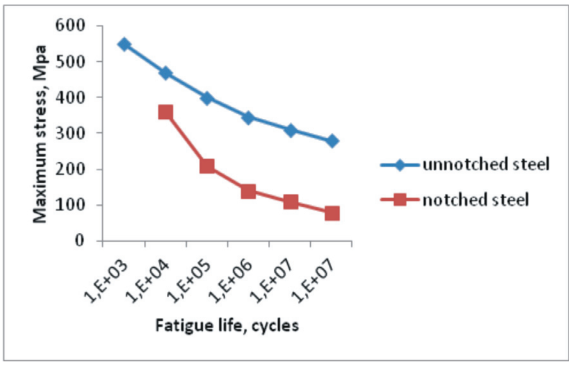

Figure 4. The effect of fatigue life on an alloy steel endurance

METHODOLOGY

This work employed data on a real production scale from a coal power plant where a superheater tube was damaged. The method consisted of ash velocity determination and the calculation of the amount of material removal. The ash velocity and the impacting angle were determined by computational fluid dynamic (CFD) simulation using PHOENICS Software. PHOENICS software is a commercial simulation package that has several modules to cater for different simulation purposes. Coal combustion simulation uses COFFUS and FLAIR modules which will be used in this work. The CFD simulation will provide velocity vector and temperature profiles in the furnace including the area near the superheater bank. The amount of material removal was calculated using procedures described by Equations 1 to 15. Parameters used for computational analysis were ash particle characteristics, type of impacting material, the amount of ash and ash velocity. The abrasiveness of the coal ash was represented by its silica content. Coal ash data were taken from one of three samples since the composition of materials in those samples are similar.

The coal power plant is a pulverized type using 20 coal inlets to provide input to the furnace. Of the 20 inlets, there were only 16 inlets being operated at one time. The pulverized coal was supplied through these inlets together with primary combustion air. The CFD simulation uses real scale power plant with the width 42.2 m, depth 34.5 m and height 70.7 m. The coal furnace was configured in modules COFFUS and FLAIR. The coal inlet had a square section with the dimension of 472.89 mm wide, 343.68 mm long and 2240.00 mm deep. Five coal inlets were mounted at each corner of the furnace at the position of 20.77, 22.42, 24.07, 27.37, 29.02 meter from the bottom, with the angle of 15o. The coal inlets were surrounded by primary and secondary air inlets, as well as oil burners for initial combustion. The construction material of the superheater tubes was of type A213-T91 which was the standard ASTM material with the pipe wall thickness 3.2 mm. The material type determined its yield stress parameter which affected the amount of mass removed by the ash particle during impact.

Simulation parameters comprised operating conditions based on design specification presented in the following list.

-	Production capacity	300 MW
-	Coal consumption	159.95 ton/hour
-	Coal calorific value (LHV)	17,250 kJ/kg (ar)
-	Primary air flowrate	317.61 ton/hour
-	Secondary air flowrate	523.78 ton/hour
-	Nominal load	255 MW
-	Steam flowrate	1025 ton/hour
-	Outlet superheated steam	17.4 MPa and 541 °C

Coal characteristics used for the CFD simulation are given in Table 1, while the coal ash characteristics are given in Tables 2, 3, and 4. Table 5 presents material characteristics of the superheater tube. Data in Tables 2 – 5 were used for erosion simulation as input to Equation 3 – 15. Table 1 shows the design specified coal which is the characteristics of coal to be used for the plant stated out in the project document (Boiler Specification, 2008). As for the actual coal used during the rupture incident, there were three coal samples available taken from three different analysis certificates (Certificate of Coal Sampling and Analysis, 2010). Coal I, Coal II and Coal III are

Table 1. Coal characteristics used for simulation

No.	Description	Symbol	Unit	Design Specified Coal	Coal Sample (Coal I)
1	Ultimate analysis as received	Car	%	46.00	44.82
2		Har	%	3.77	3.28
3		Oar	%	13.90	12.95
4		Nar	%	1.00	0.60
5		St.ar	%	0.33	0.20
6		Aar	%	5.00	3.49
7	Total moisture	M t.ar	%	30.00	34.66
8	Volatile content	Vdaf	%	53.00	33.95
9	LHV (Low Heating Value)	Qner.ar	kJ/kg	17250	17425
10	Grindability	HGI		>50	62
11	Coal consumption		ton/hour	159.95	±158

Table 2. Ash size distribution (Certificate of Coal Sampling and Analysis, 2010)

No.	Size distribution	Weight % Coal I
1	Pass 70 mm sieve	100
2	Pass 50 mm sieve	95.33
3	Pass 32 mm sieve	79.69
4	Pass 2.38 mm sieve	18.76
	Average sieve, mm	35.66

Table 3. Coal ash characteristics

No.	Description	Symbol	Unit	Value
1	Ash particle diameter in average calculated from the average sieve (35.66 mm) on Table 2	d_p	meter	0.0005
2	Ash particle density (Mbazi et al, 2006)	ρ_p	kg/m^3	481
3	Particle shape factor (Mbazi et al, 2006)	c		3

Table 4. Main material in coal ash

No.	Material	Weight % Design specified coal	Weight % Coal I
1	SiO_2	11.7	46.54
2	Al_2O_3	54	17.91
3	Fe_2O_3	12	13.62

the actual characteristics of coal that have been used in the plant. Since the composition of the material in the coal samples is similar, only one set of data was used for this study that is Coal I data set. It can be seen that the coal that have been used in the plant does not differ very much from the design specified coal. However, the design specification uses coal with the silica content in the coal ash at 11.7 %. The value is much lower than that of the silica content in the ash from actual coal burned in the plant. See design specified coal and Coal I sample in Table 4. While the alumina content of the design specified coal was much higher than that of the actual coal. This study will focus on the silica content only, since it is more abrasive than the other materials that contribute the coal ash.

Ash diameter was determined using the percentage of particles that passed through a series of mesh sieves. The analysis used series 70, 50, 32 and 2.38 mm sieves which correspond to 0.210, 0.297, 0,595 and 8 mm particle size. Table 2 shows the distribution of the ash particle diameter. It was found that the average particle size is 35 mm sieve which is equivalent to 0.5 mm in particle diameter. This work uses the average particle size diameter given in the coal data analysis.

The main material contained in the ash consists of SiO_2, Al_2O_3, and F_2O_3 which is shown in Table 4. The actual coal has different silica content than that of the design specified coal.

RESULTS AND DISCUSSIONS

COFFUS modul of the PHOENICS Software was used to model the coal furnace on a real scale with the grid of 60*60*120 towards X,Y and Z axis respectively (see Figures 5 and 6). Figure 5 is the coal furnace model showing the coal inlets, combustion zones, superheater, reheater and the outlet. Figure 6 shows the grids or the number of cells that was used for running the simulation. The number of sweeps for the simulation was 600. Coal inlets were positioned at 15o tangential plane and 20° upward swing. Combustion products flowed from the burning region at the coal inlets upward towards the superheater bank, turned direction and into the reheater bank. Flue gas outlet was positioned near the bottom of the rightside region after the air preheater. Combustion products consisted of gases, dusts, soots and ash particles.

The results of COFFUS simulation show flow distribution with velocity vector (Figures 7 and 8) and concentration distribution of ash (Figure 9).

Table 5. Material strength of superheater tube (ASTM-A213-T91-ASME-SA213-T91-specification)

No.	Description	Symbol	Unit	Design
1	Material type			alloy steel type A213-T91
2	Yield strength	σy	MPa	220
3	Tensile strength		MPa	415
4	Wall thickness	δ	mm	3.2

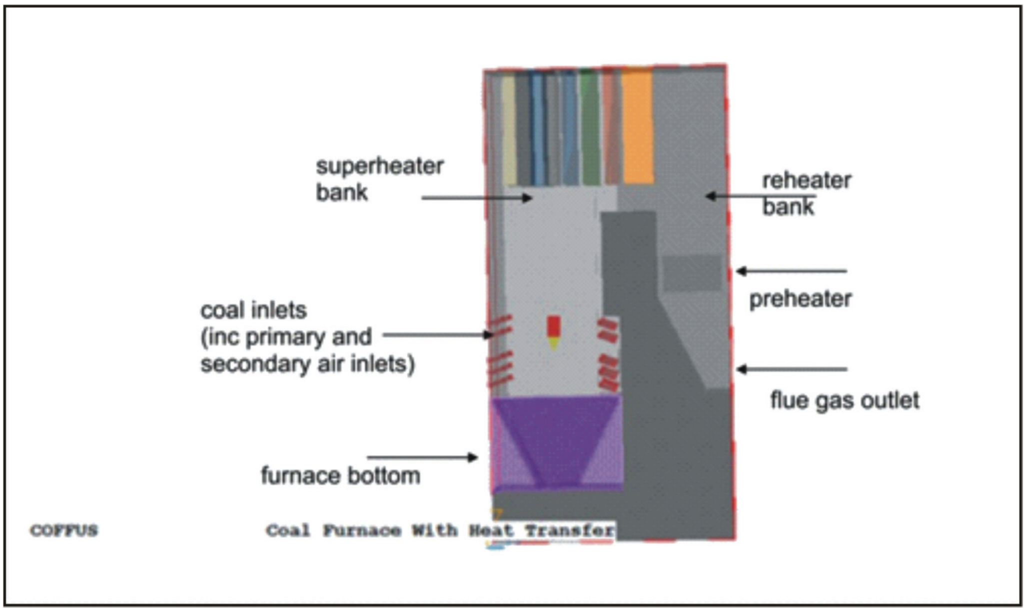

Figure 5. Coal furnace configuration in PHOENICS Software

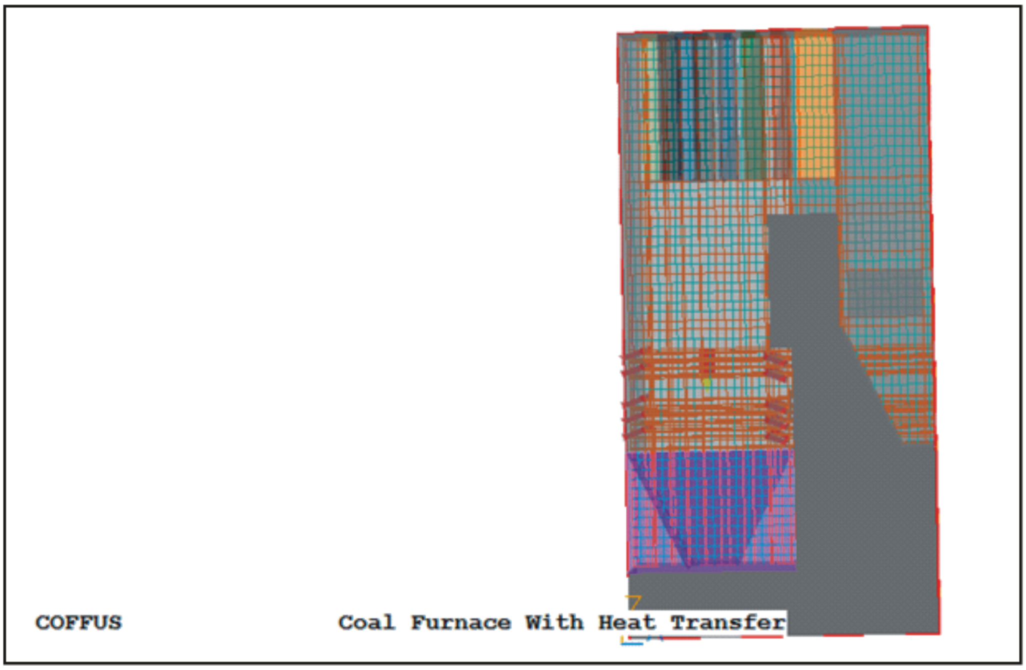

Figure 6. Coal furnace configuration with simulation grids

The magnitude of the velocity is shown in colors from blue to red where blue indicates low values and red shows high values.

Figures 7 and 8 show that the combustion product flow velocity near the superheater bank varies from 1 to 20 m/s with the impacting angle also varies from 0° vertical relative to the position of superheater to 90° which is perpendicular to the superheater. From the ash concentration distribution (Figure 9) it can be seen that ash produced from the combustion is found in high concentration around superheater bank or at the upper part of the furnace. This is quite agreeable with the op-

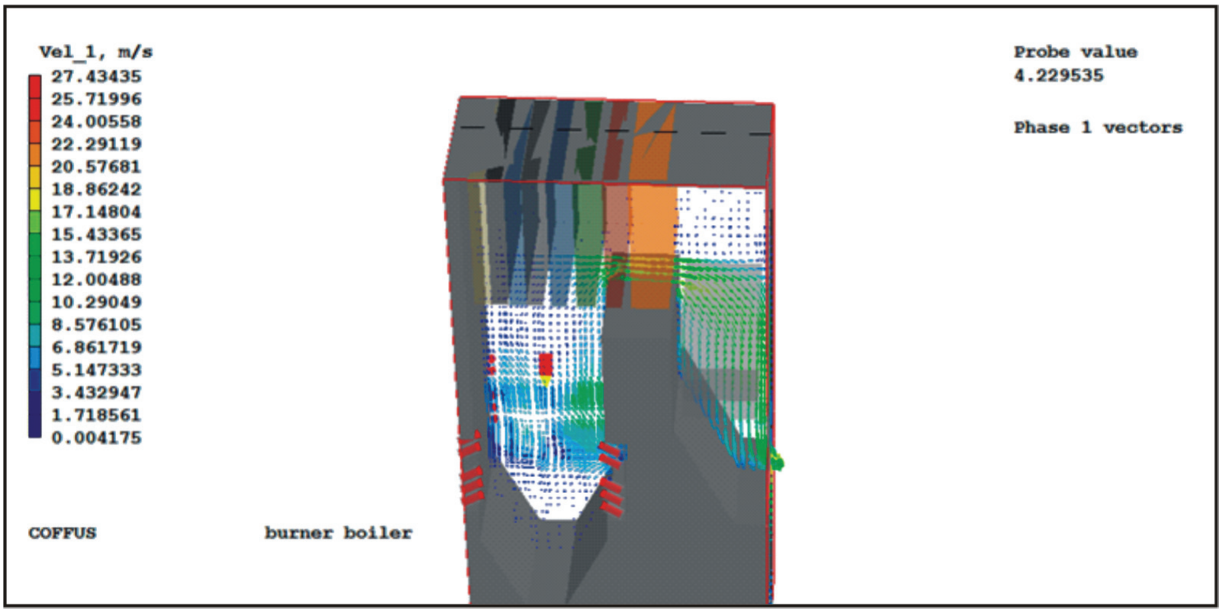

Figure 7. Velocity vector distribution in the coal furnace

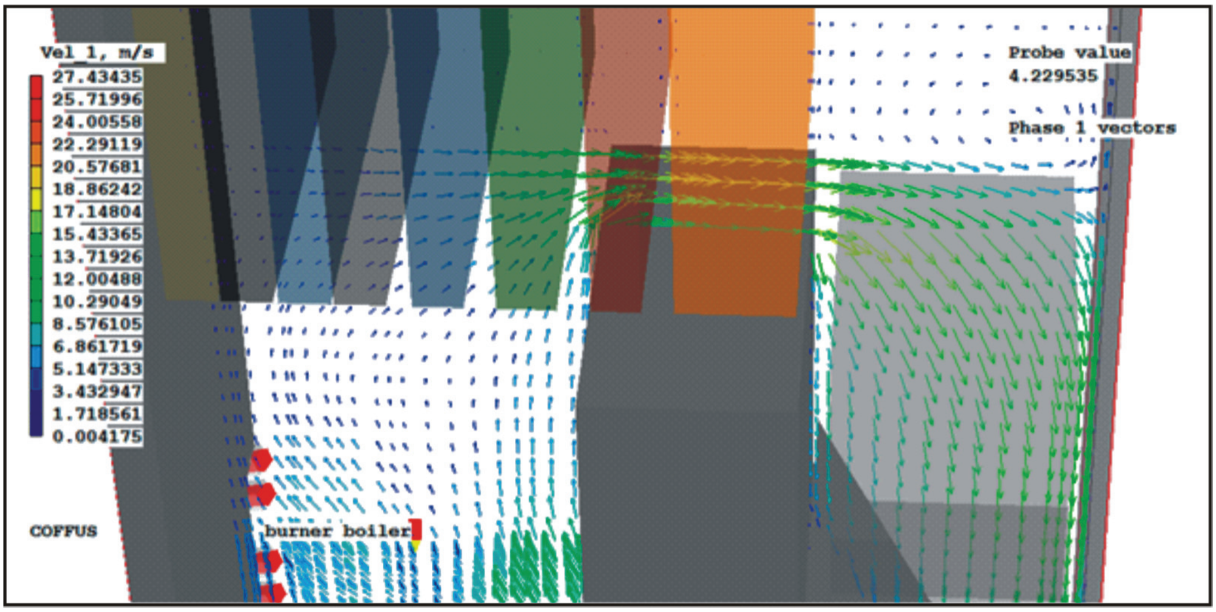

Figure 8. Velocity vector distribution near the superheater bank

eration of the boiler where flue gas and combustion products are brought into the superheater and reheater banks to provide heat to the steam. The concentration of the ash is denoted in fraction.

FLAIR simulation on fire and smoke in the furnace resulting in the following distribution as shown in Figure 10 where smoke particles are found within the upper part of the furnace similar to ash distribution. The smoke particles are measured in fraction relative to the other gasous products. The highest concentration of the smoke particles is at 0.3.

Based on the impacting angle and material data of each abrasive particle, and using Equation 3 and 4, the degree at which the maximum erosion takes place is found to be at 17° with the amount

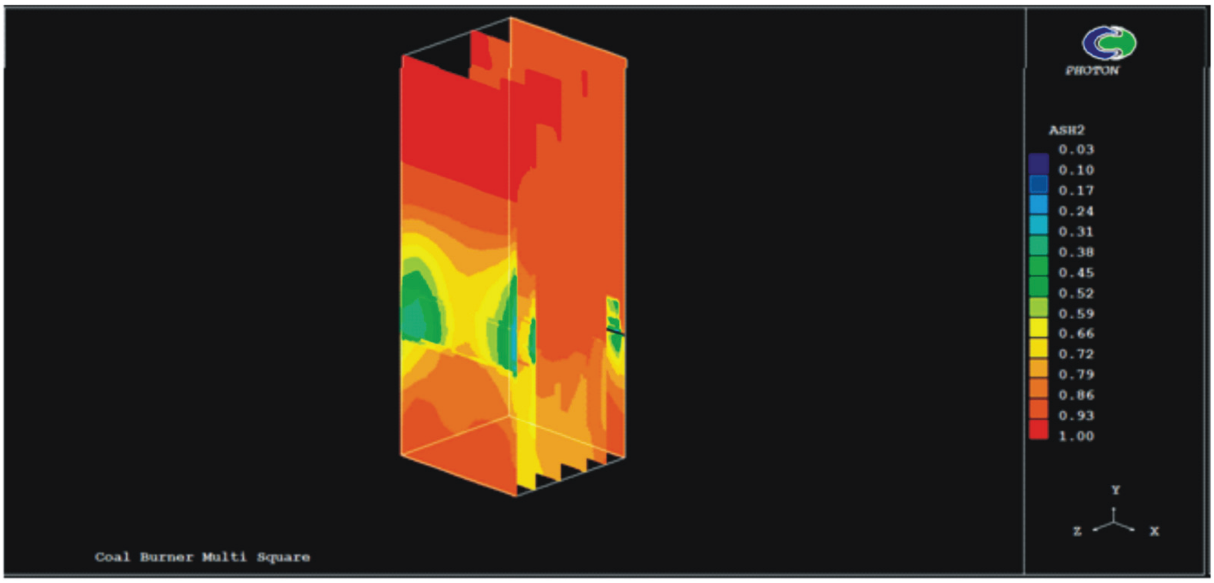

Figure 9. Distribution of ash concentration in a coal furnace

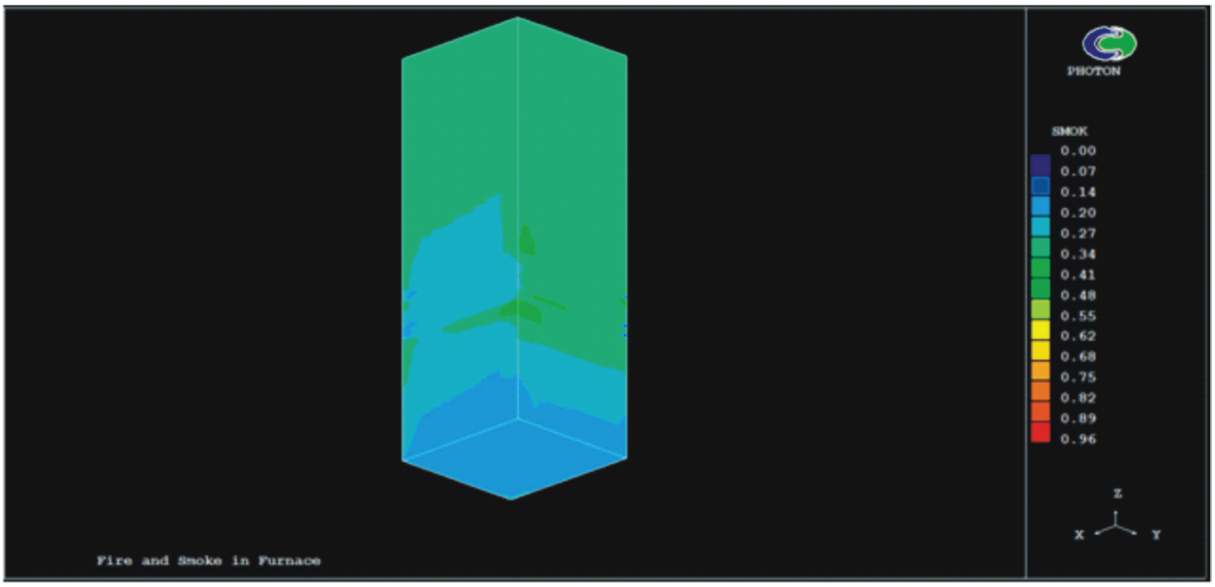

Figure 10. Smoke particle distribution in a coal furnace

of removal is 1.6 * 10-7 mg for each ash particle (Figure 11). The trend of the graph is in agreement with experiments done by other researchers although the value of the impacting angle and the amount of mass removed is different due to the differences in the material being studied, as shown in Table 6 below. The impacting angle (17°) is an indicator for maximum level of impact and further used to determine the amount of mass removal of the impacting material by varying the velocity and and abrasiveness of the ash particles.

The amount of mass removed by the impact is varied according to the particle velocity. The amount was calculated using Equations 6 to 15. It can be seen that the amount of mass removed increases with the increasing velocity as shown in the following diagram (Figure 12). The figure shows the amount of mass removal using ash content of 46.54 % from Coal I. At the maximum ash velocity taken from the CFD simulation which is 20 m/s and 500 micron average diameter, the amount of mass removal is 0.0045 mg/kg ash.

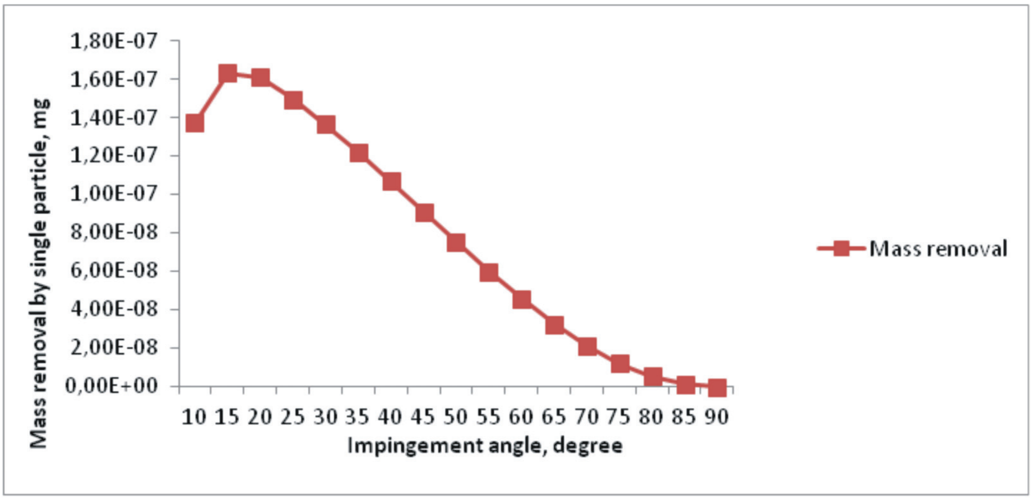

Figure 11. Mass removal by impacting angle

Table 6. Impacting angle of maximum erosion

Researchers	Impacting angle that cause maximum erosion
Finnie (1960)	
Material: aluminium, copper and steel with carbide grains	18 – 20°
Mbabazi (2004)	
Material: mild steel with coal ash	30°
This work (alloy steel with coal ash)	17°

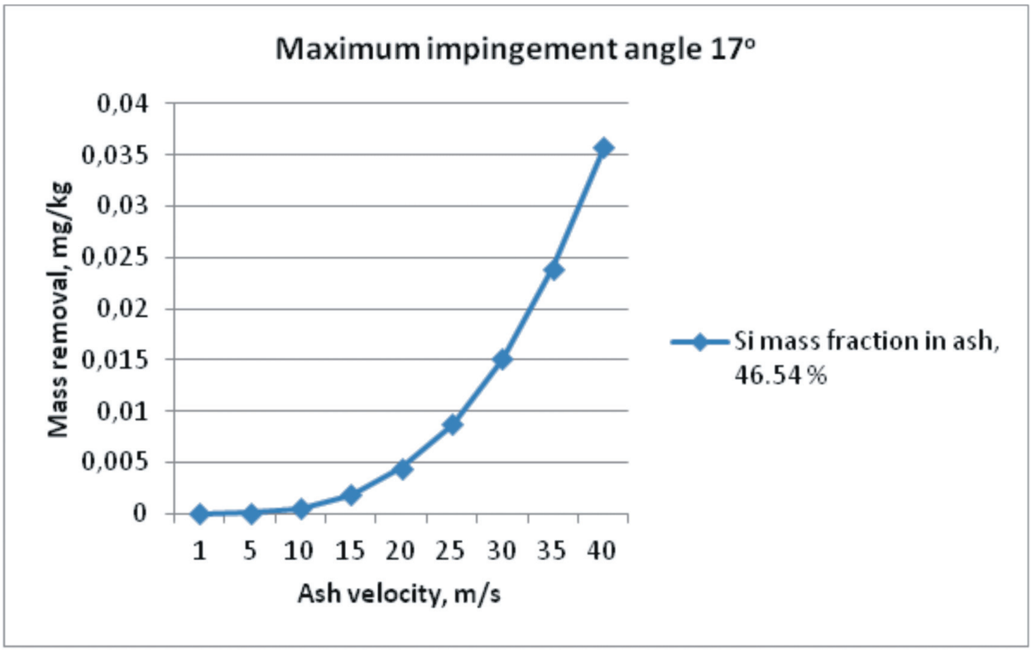

Figure 12. The amount of material removal depending on ash velocity at impingement angle 17°, mg/kg ash

The amount of abrasive grains affects the amount of mass removal. If the amount of abrasive grains increases, then the amount of mass removal will also increase. Figure 13 shows the amount of mass removal according to differences in the amount of abrasive or ash material. It can be seen that the mass removal maximum was at 17°.

The maximum penetration for each particle velocity calculated using Equation 9 is presented in Figure 14. It shows that if the velocity of the finest particle (ξ = 210 micron) is beyond the velocity range for instance at 40 m/s, the maximum penetration is only reached 0.04 mm compared to the wall thickness 3.2 mm. This shows that

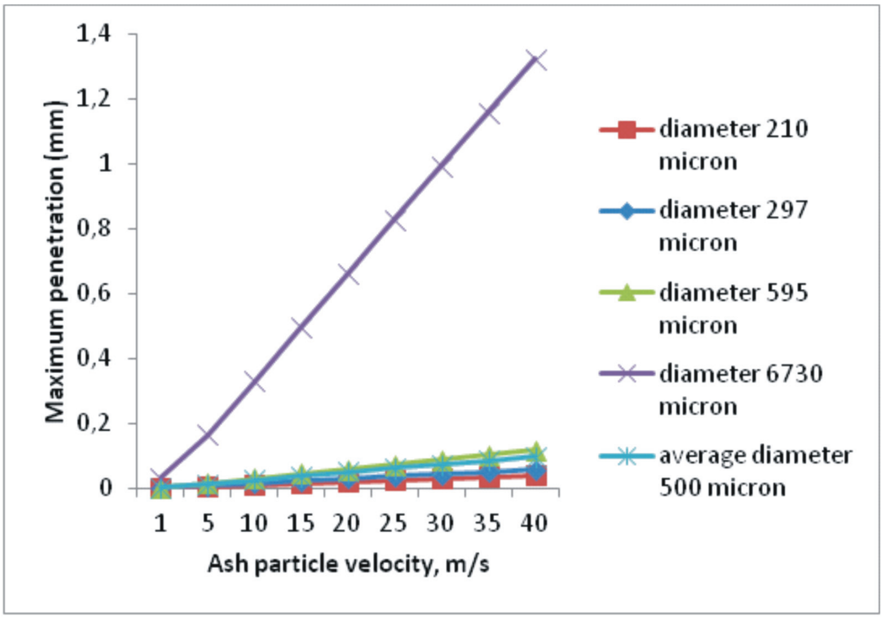

Figure 13. Differences in the amount of mass removal in relation with the impacting degree

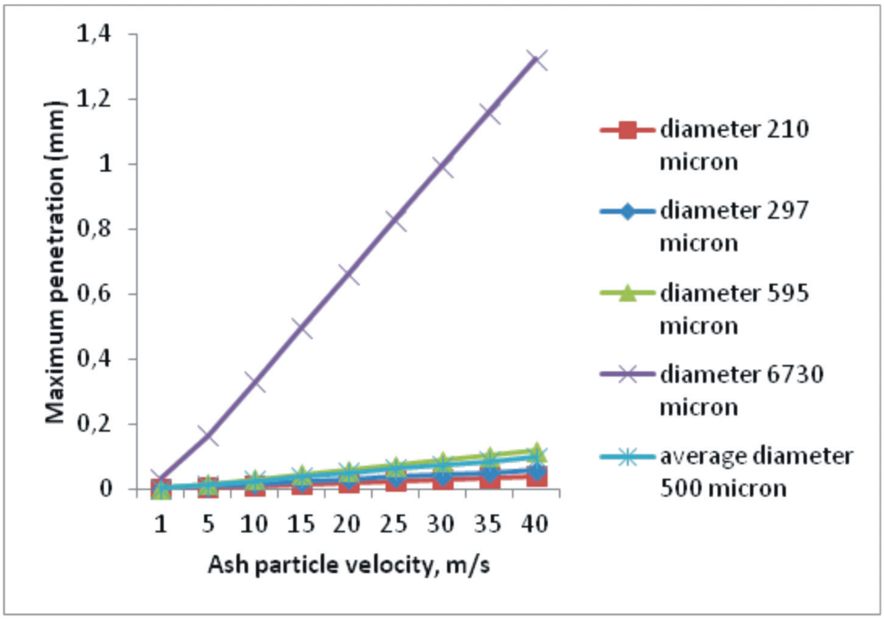

Figure 14. Maximum penetration of ash particle with different velocity and different particle diameter

the effect of erosion is very small compared to the time of pipe rupture. For maximum velocity being examined in this study, that is 40 m/s, the percentage of wear is about 1.25 % of the material thickness. The figure also shows that particle diameter affects the amount of penetration into the impacting material. If the diameter is larger then the maximum penetration is also bigger which can reach 1.4 mm at maximum velocity. Based on the particle size distribution the average particle diameter is around 500 micron. At the velocity of 20 m/s, this results in 0.049 mm of maximum penetration which is about 1.53 % of the wall thickness.

The percentage of silica content in coal ash affects the amount of mass removal as shown in Figure 15. the higher the silica content, the higher the amount of mass removal. This is due to the abrasive characteristics of the silica in ash. Compared to the ash content of the design specified coal, the ash content of the actual coal is much higher, therefore, the amount of mass removal caused by this coal is also several folds. Figure 15 shows the comparison of the ash with silica content 11.7 % (design specified coal) with that of ash with silica content 46.54 % (actual coal). The effect of mass removal can be seen only when the velocity is above 7 m/s. Coal ash with low silica content has an insignificant effect on the amount of mass removal. While ash velocity in combination with the amount of silica plays an important role shown by the exponential increase of the amount of mass removal. This result may suggest that it is advisable for the plant operator to use coal with low silica content. However, this is not possible from the practical point of view since we have not been able to find coal of that type.

The effect of the material fatigue was examined by reducing the yield stress of the material down to 80, 50 and 30 % respectively. The amount of mass removal will be different if the Si content in ash is different as shown in Figures 16 and 17. The following graph (Figure 16) shows that if the material has 30 % fatigue which has longer life cycles, the amount of mass removal is increased. The calculation used ash with a silica content of 46.54 % and average ash diameter 500 micron. If the calculation used silica content 11.7 %, then the amount of mass removal is reduced significantly (Figure 17), that is about one 1000th of the 46.54 %. This differences suggest that the amount of silica in ash plays an important role in boiler or superheater tube erosion.

If the yield strength was varied, then the amount of mass removal increased exponentially (Figure 18). This is in corresponding with the reducing of the material endurance as given in Equation 15. Equation 16 represents the link between the material strength and the amount of removal.

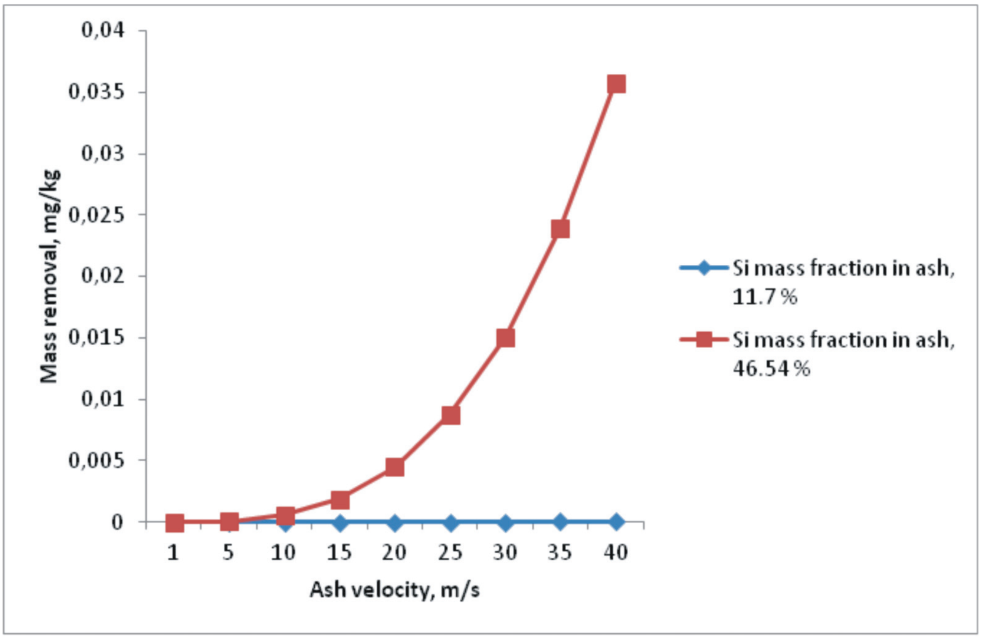

Figure 15. The effect of silica content (in percent) in coal ash on the amount of mass removal

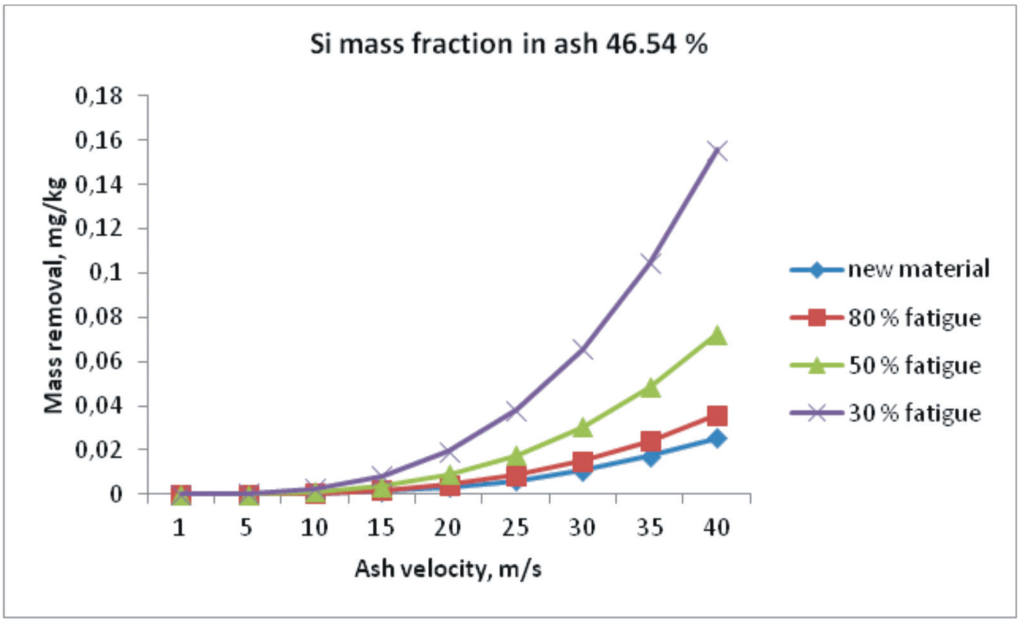

Figure 16. The effect of material yield stress on the amount of mass removal using average ash size 500 micron and silica content 46.54 %

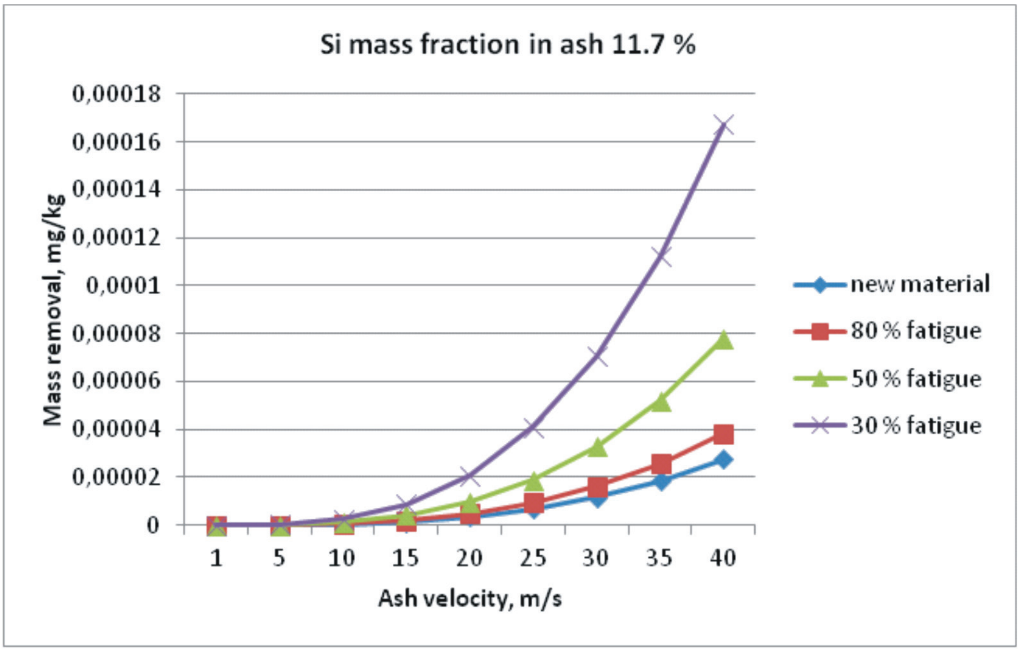

Figure 17. The effect of material yield stress on the amount of mass removal using average ash size 500 micron and silica content 11.7 %

$y = 0.0013e^{0.7543x}$ .... (16)

The exponential relationship suggests that the failure occured if the material had undergone millions life cyles in which the endurance limit of the material had been achieved. Therefore if the material used in its initial yield strength, a sudden failure and burst of pipe is almost unlikely. However there are other factors that may affect the untimely fracture as suggested by the evidences from the failed superheater tubes listed below.

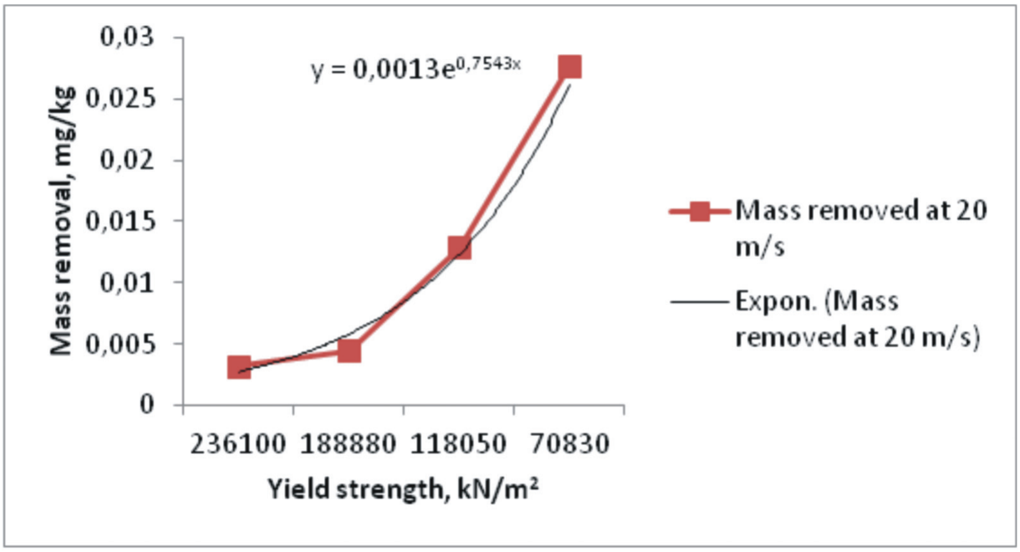

Figure 18. The relation between the amount of mass removal with the strength of the material at velocity 20 m/s using average size 500 micron

There was only one tube that failed. This indicates that if ash erosion caused the thinning of the tube wall, then it must also inflict other tubes.

It has been found out that the failed tube was clogged by dirts in the form of soot and ash. It had undergone overheating which caused fracture at the bend of the tube.

As an overall, it was observed that welding and installation of the superheater tubes were sub standard as indicated by further investigation of the power plant.

The quality of the construction material for this plant might be intended to be used for low silica ash according to the project document. However the current coal cannot satisfy the requirements.

CONCLUSIONS

The wear of superheater material is predictable and can be measured during the power plant operation. The model and simulation used for this study of ash erosion on superheater pipes show that the wear of the material was affected by the coal type which related to the amount of ash, ash diameter, ash particle velocity, silica content in ash, impacting angle and the type of impacting material. The higher the amount of ash, ash particle velocity, ash diameter and the silica content in ash, the higher the amount of mass removal of the impacting material. If the impacting angle was more slanting, the amount of mass removal was also high. The type of impacting material was varied depends on its yield strength. For these particular coal ash and plant design operating parameters, the maximum effect of the ash erosion was only 1.25 % of mass removal from the impacting material, which should not cause immediate failure to the pipes. The study concluded that ash erosion was not the sole factor of the sudden pipe burst. For an incident of untimely superheater failure, especially during initial operation of the power plant, there were other factors involved especially that relate to the use of construction material as suggested by the evidences from the failed pipe. Physical observation has indicated that there was an obstruction at the bend of a superheater tube due to accumulation of dirts. This condition caused overheating and sudden burst. For further understanding on the material quality, metallurgical examination of the material at microscopic level was required. It is possible that the material used has already undergone microstructural changes and the fatigue level had been achieved and thus could not retain its initial elasticity. The fatigue level will be achieved when the material has undergone a certain number of life cycles shown by low yield strength.

ACKNOWLEDGMENT

The author would like to express her gratitude to PT Indonesia Power for providing data for the study of ash erosion on boiler tubes of coal fired power plant.

REFERENCES

ASTM-A213-T91-ASME-SA213-T91-specification

Boardman, B., 1990. Fatigue Resistance of Steels, *ASM Handbook*, Volume 1: Properties and Selection: Irons, Steels, and High-Performance Alloys, p. 673-688.

Certificate of Coal Sampling and Analysis, (2010)

Finnie, I., 1960. Erosion of surfaces by solid particles, *Wear 3*, p. 87-103.

Finnie, I. and McFadden, D.H., 1978. On the velocity dependence of the erosion of ductile metals by solid particles at low angles of incidence, *Wear*, 48, p . 181 - 190

Gong, Y., Zhong, J. and Yang,Z.G., 2010. Failure analysis of bursting on the inner pipe of a jacketed pipe in a tubular heat exchanger, *Materials and Design 31*, p. 4258–4268.

Mbabazi, J.G., Sheer, T.J. and Shandu, R., 2004. A model to predict erosion on mild steel surfaces impacted by boiler fly ash particles, *Wear 257*, p. 612–624

Mbabazi, J.G. and Sheer, T.J., 2006. Computational prediction of erosion of air heater elements by fly ash particles, *Wear 261*, p. 1322–1336

Port, R.D. and Herro, H.M., 1991. *The Nalco Guide to Boiler Failure Analysis*, Nalco Chemical Company, McGraw-Hill, Inc., New York, p. 29-31.

Boiler Specification, 2008. *Project Document Equipment Specification*.

Purbolaksono, J., Ahmad, J., Khinani, A., Ali, A.A. and Rashid, A.Z., 2010. Failure case studies of SA213-T22 steel tubes of boiler through computer simulations, *Journal of Loss Prevention in the Process Industries 23*, p. 98–105.

Rahimi, M., Abbas Khoshhal, A. and Shariati, S.M., 2006. CFD modeling of a boiler's tubes rupture, *Applied Thermal Engineering 26*, p. 2192–2200.

Sandberg, J., Fdhila, R.B., Dahlquist, E. and Avelin, A., 2011. Dynamic simulation of fouling in a circulating fluidized biomass-fired boiler, *Applied Energy 88*, p. 1813–1824.

Vuthaluru, H.B. and Vuthaluru, R., 2010. Control of ash related problems in a large scale tangentially fired boiler using CFD modelling, *Applied Energy 87*, 1418–1426.

NOMENCLATURE

c	ash particle shape factor equal to 3 for a sphere
d_p	ash particle diameter
h	penetration equals h
H_v	Vickers hardness number of the impacting material
K	the ratio of vertical to horizontal force components, for abrasive material ~ 2
m and m_p	ash particle mass
M	the total mass of ash particles
p	atmospheric pressure
Q	the volume of material removed by a single ash particle
V	initial velocity of ash particle
x	the mass fraction of silica contained in the ash
y_t	leaving velocity of ash particle

Greek letters

α	cutting angle
ε	total mass removal
ϕ	impact direction
ρ_p	ash particle density
ρ_m	the density of the target material
σ_y	the yield stress of the target material
ψ	constant value for depth of cut, for abrasive material ~ 2